Available online at www.sciencedirect.com
ScienceDirect
Journal of Power Sources 159 (2006) 509–513
JOURNAL OF POWER SOURCES
www.elsevier.com/locate/jpowsour

A more active Pt/carbon DMFC catalyst by simple reversal of the mixing sequence in preparation

Jianhuang Zeng, Jim Yang Lee *, Weijiang Zhou

Department of Chemical and Biomolecular Engineering, National University of Singapore, 10 Kent Ridge Crescent, Singapore 119260, Singapore

Received 15 July 2005; accepted 5 November 2005
Available online 20 December 2005

Abstract

Vulcan XC-72 carbon-supported Pt nanoparticles are prepared by a conventional route, i.e. by adding $NaBH_4$ solution to a carbon slurry of a Pt precursor salt (Pt-1/C); and by a simple reversal of the mixing sequence in which the Pt precursor salt was added to a carbon slurry of $NaBH_4$ (Pt-2/C). Transmission electron microscopy and X-ray photoelectron spectroscopy are used to obtain information on the particle size and size distribution, as well as on the surface oxidation state of the Pt nanoparticles. From cyclic and anodic CO-stripping voltammetric evaluation of catalyst activity for the methanol oxidation reaction (MOR) in acidic solution at room temperature, the Pt-2/C catalyst, which has none of the attributes generally associated with a good Pt catalyst (small particle size, narrow size-distribution, high metal dispersion, low Pt oxidation state), demonstrated higher specific activity and improved CO tolerance than the conventionally prepared Pt-1/C, which has all the common features of a good Pt catalyst. It is concluded that the higher activity of Pt-2/C is linked to its surface oxygen species, which is present in greater abundance and in a more accessible form for reaction with the strongly adsorbed CO-like intermediates.

Keywords: Platinum nanoparticles; Methanol oxidation reaction; CO tolerance; Specific activity; Catalyst; Carbon slurry

1. Introduction

The catalytic electro-oxidation of methanol at room temperature is the principal feature of direct methanol fuel cells (DMFCs), which are well poised to become the fastest growing next-generation mobile power source [1]. The catalysts used are invariably Pt based and rendering the Pt into a highly active form is an important design consideration. Despite ongoing debates on the optimum size of the Pt particles and the role of metal–support interactions, it is generally believed that a good carbon-supported Pt catalyst should have some predetermined features such as small particle size, narrow particle size distribution, a high state of dispersion on the support, and Pt in the fully-reduced metallic state. This study presents data contrary to these selection criteria.

Many methods have been reported for the preparation of carbon-supported Pt catalysts, among which the chemical reduction of Pt precursors is probably the most common. The conventional route to the formation of Pt particles is to introduce the reducing agent dropwise to a Pt precursor solution, or a carbon slurry of the Pt precursor solution [2–4]. Reasonably good control of particle size, particle size-distribution and the state of dispersion on the carbon support can often be accomplished by this simple technique [5]. In this work, an unusual route to Pt formation route has been deliberately adopted, namely, addition of the Pt precursor solution to a carbon slurry of the reducing agent $NaBH_4$. The resulting carbon-supported Pt catalyst has a broader particle size-distribution, a less-than-uniform metal dispersion, and a higher content of oxidized Pt on the particle surface. Despite these features, the catalyst has performed well for temperature methanol oxidation at room temperature, in terms of catalyst specific activity and CO tolerance.

2. Experimental

Chloroplatinic acid (H_2PtCl_6) was purchased from Aldrich. Sodium borohydride ($NaBH_4$), sulfuric acid (95–97%) and methanol were supplied by Merck. The carbon support was

* Corresponding author. Tel.: +65 6874 2899; fax: +65 6779 1936.
E-mail address: cheleejy@nus.edu.sg (J.Y. Lee).

0378-7753/$ – see front matter © 2005 Elsevier B.V. All rights reserved.
doi:10.1016/j.jpowsour.2005.11.049

Vulcan XC-72 (measured BET surface area of 228 $m^2\,g^{-1}$ and average particle size of 40–50 nm) from Cabot. All chemicals were used as received without further purification. De-ionized water was employed throughout the study.

Two Pt catalysts were prepared on Vulcan XC-72 carbon at a 20 wt.% of metal loading.

(1) Pt-1/C ('control'): 2 ml 50 mM H_2PtCl_6 was mixed with 120 ml of de-ionized water that contained a calculated amount of Vulcan XC-72 carbon, followed by 30 min of sonication. A 2 ml sample of a solution containing 100 mg $NaBH_4$ was added dropwise to the carbon suspension with vigorous stirring at room temperature. Stirring was continued overnight before the solid phase was recovered by filtration and then washed copiously with water. The recovered solid was dried under vacuum at room temperature overnight.
(2) Pt-2/C: 120 ml of de-ionized water containing a calculated amount of Vulcan XC-72 carbon was sonicated for 30 min in an ultrasonic bath to form a carbon slurry. Hundred milligrams of $NaBH_4$ was immediately added together with 2 ml of 50 mM H_2PtCl_6. The rest of the preparative procedures were the same as those used for the preparation of Pt-1/C.

X-ray powder diffraction (XRD) patterns of the catalysts were recorded with a Rigaku D/Max-3B diffractometer (Shimadzu) that used Cu Kα radiation (λ = 1.5406 Å). The 2θ angles were scanned from 20° to 85° at 2° min^{-1}. The diffraction data was curve-fitted by a least-squares program that was provided by the equipment manufacturer. Elemental compositions, of the Pt loading in particular, were determined by an EDX analyzer attached to a JEOL MP5600LV scanning electron microscope (SEM) that operated at 15 kV. Information on particle size, shape and size distribution was obtained with a JEOL JEM2010 transmission electron microscope (TEM) at 200 kV. X-ray photoelectron spectra were obtained from an ESCALAB MKII spectrometer (VG Scientific) using Al Kα radiation (1486.71 eV). Spectral correction was based on the graphite C1s level at 284.5 eV. The vendor-supplied XPSPEAK version 4.1 was used to deconvolute the XPS data; fixed half widths and fixed spin orbit splitting were used in the first trials.

An Autolab PGSTAT12 potentiostat/galvansotat, and a standard three-electrode electrochemical cell were used to evaluate the catalysts by cyclic voltammetry. The working electrode was a vitreous, glassy-carbon disc electrode (5 mm diameter) that was cast with a catalyst ink in Nafion solution to a Pt loading of 18 μg cm^{-2}. A Pt gauze and a saturated calomel electrode (SCE) were used, respectively, as the counter electrode and the reference electrode to complete the circuit. The electrolytes were 0.5 M H_2SO_4 and 1 M CH_3OH in 0.5 M H_2SO_4. A potential window of −0.2 to 1 V (with respect to SCE) was scanned at 20 mV s^{-1} until a stable response was obtained before the voltammograms were recorded. The CO tolerance of the catalysts was evaluated by anodic stripping of adsorbed CO. This was done by saturating 0.5 M H_2SO_4 with 10% CO in Ar while the working electrode was held at −0.15 V for 30 min. The passage of CO was then stopped and the electrolyte was thoroughly purged with high purity Ar. The CO-stripping voltammograms were collected over the −0.2 to 1 V potential window starting from −0.15 V.

3. Results and discussion

The Pt loadings in Pt-1/C and Pt-2/C were about 20 wt.% as determined by EDX. Transmission election micrographs and the corresponding particle size-distributions of the two catalysts (Pt-1/C and Pt-2/C) are shown in Fig. 1. The Pt particles in Pt-1/C had a number-averaged particle size of 4.1 nm (σ = 1.7 nm) and were fairly uniformly distributed on the carbon support (Fig. 1(a)). By contrast, the Pt particles in Pt-2/C followed a bimodal distribution, with a mean of 5 nm for the larger particles and a mean of 0.8 nm for the smaller ones. Isolated Pt nanoparticles can also be found outside the carbon support, which is not the case with Pt-1/C. Low magnification TEM images (data not shown) of Pt-2/C also showed a few XC-72 flakes to be completely devoid of Pt. The difference between the two catalysts can be understood in terms of a series reaction scheme in which particle nucleation and growth are consecutive reactions with large particles as the final product. In the preparation of Pt-1/C, the addition of $NaBH_4$ to $PtCl_6^{2-}$ creates heterogeneity in the Pt source concentration (reacted versus un-reacted) which favours the formation of the end product [6]. Nucleation probably occurs preferentially on the carbon support by the reaction between adsorbed $PtCl_6^{2-}$ anions and incoming reducing agent $NaBH_4$ [7]. Further addition of $NaBH_4$ results in $PtCl_6^{2-}$ reduction and particle growth because the creation of new nuclei is not energetically favourable in the solution phase. In the case of Pt-2/C, where $PtCl_6^{2-}$ is the limiting reactant among an excess of $NaBH_4$, nucleation has to be initiated in the solution phase, and the Pt particles formed are subsequently deposited on the carbon support. Since the particles are not formed synchronously, their deposition on the carbon support (and stabilization against further growth as such) is a stochastic process, which results in a wide range of particle sizes. Some particles might also be deposited without being captured by the carbon support.

The XRD patterns of the catalysts are shown in Fig. 2. The broad reflection centred about 2θ = 25° is the graphite (0 0 2) diffraction from the carbon support [8]. For both catalysts, strong diffraction peaks at Bragg angles of 39.8°, 46.3°, 67.5° and 81.3° are detected and can be indexed to the (1 1 1), (2 0 0), (2 2 0) and (3 1 1) planes of face centred cubic (fcc) Pt.

Wide-scan XPS spectra of Pt-1/C and Pt-2/C reveal only the presence of C, O and Pt, without any trace of boron. The Pt 4f spectra of Pt-1/C and Pt-2/C are given in Fig. 3. In Fig. 3(a), the more intense doublet at 71.44 and 74.74 eV is a signature of metallic Pt, while the less intense doublet at 72.84 and 76.04 eV is often assigned to oxidized Pt in the divalent state such as PtO and Pt $(OH)_2$ [9]. The Pt 4f spectrum of Pt-2/C (Fig. 3(b)) can be deconvoluted into three doublets, with the doublet at 71.71 and 75.04 eV to Pt(0), the doublet at 72.71 and 76.04 eV assignable to Pt(2), and the doublet at 73.83 and 78.20 eV to Pt(4) [10,11]. One would have expected a higher Pt(0) content

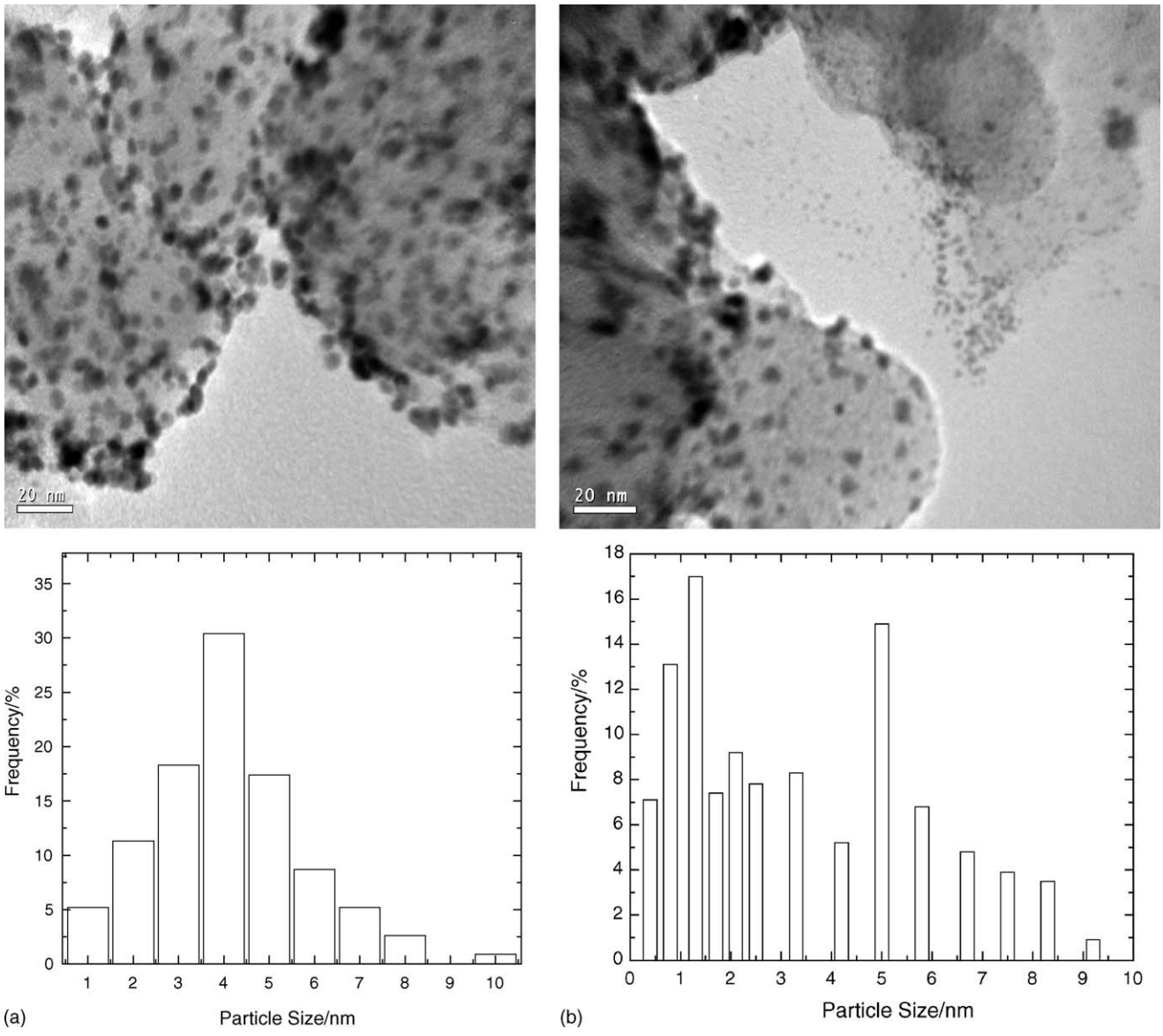

Fig. 1. Transmission electron microscopic images and histograms of particle-size distributions for (a) Pt-1/C and (b) Pt-2/C.

in Pt-2/C because the Pt particles there are formed in a more reducing environment of excess $NaBH_4$. In fact, the percentages of Pt(0) in the catalysts calculated from the respective integrated intensities show the opposite results (78% in Pt-1/C and 52% in Pt-2/C). The O:Pt ratios from the same XPS spectra are similarly higher, at 12:1 for Pt-1/C and 17:1 for Pt-2/C. Our hypothesis is that the Pt particles in Pt-2/C might have been formed in a more reduced state initially but some of them were also at the same time more oxidizable because of their small size (smaller than 1 nm in Fig. 1(b)).

The CO-stripping voltammograms of the two catalysts are compared in Fig. 4. The current density is normalized by the electrochemical surface areas (ECSA) measured from hydrogen sorption voltammograms according to the standard technique [12]. In general, the voltammetric features are in good agreement in with those reported in the literature [13]. Compared with Pt-1/C, Pt-2/C has a very thick double-layer region, which suggests a higher content of oxides in the surface layer [14]. This electrochemical feature agrees well with the XPS data that show a higher content of Pt oxides in Pt-2/C. The CO-stripping voltammogram of Pt-1/C is dominated by a peak at 0.56 V that is skewed on the low potential side. By contrast, the CO-stripping voltammogram of Pt-2/C has two conjoining peaks at 0.45 V (peak 1) and 0.54 V (peak 2), both shifted negatively compared with Pt-1/C. This indicates more facile CO removal and hence improved CO tolerance in practice. In addition, a pre-oxidation wave is also detected at around 0.20 V and this could be due to the oxidation of physisorbed CO. The onset oxidation potentials are 0.16 V for Pt-2/C, and 0.27 V for Pt-1/C. The integrated charge for CO oxidation per cm^2 of ECSA, which reflects the completeness of CO removal, is also higher in Pt-2/C. The two anodic stripping peaks for Pt-2/C are likely to correspond to the

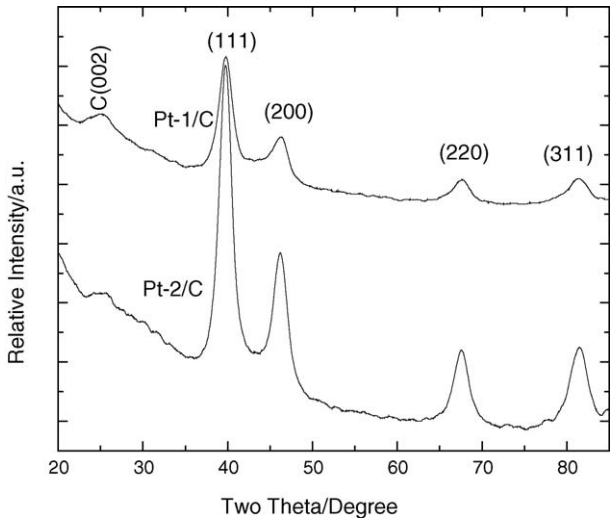

Fig. 2. X-ray diffraction patterns of Pt-1/C and Pt-2/C.

removal of adsorbed CO on Pt sites at different oxidation states. The more oxidized Pt-2/C may have some O atoms entrenched in the sub-surface region, which contribute to CO removal on the first anodic scan.

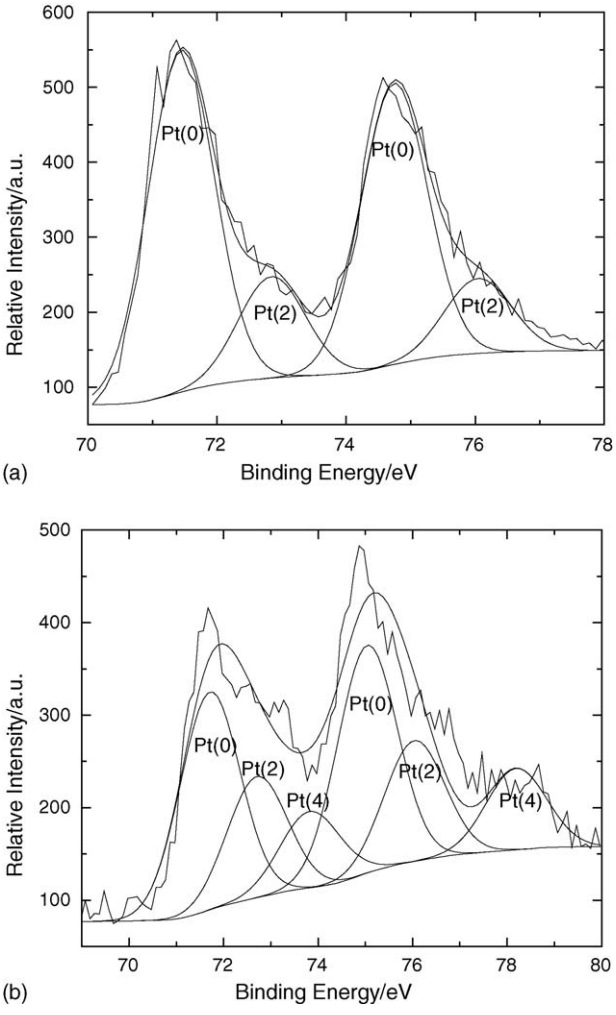

Fig. 3. Pt 4f XPS spectra of (a) Pt-1/C and (b) Pt-2/C catalysts.

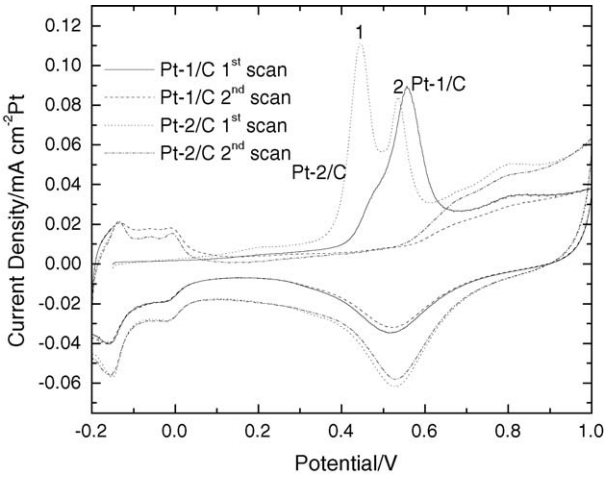

Fig. 4. Room temperature CO-stripping cyclic voltammograms of catalysts in 0.5 M H_2SO_4 (scan rate = 20 mV s^{-1}).

To prove the existence of deeply trapped and contributory oxygen species, the potential was biased at −0.35 V for various lengths of time in Ar-purged electrolyte [11] before the anodic stripping of CO. While the CO-stripping voltammogram after 3 h of polarization at −0.35 V shows only marginal changes, appreciable decreases in the overall current density and the peak height at 0.45 V are observed after a total of 17 h of polarization (Fig. 5). The CO-stripping voltammograms of Pt-1/C after the potential is biased at −0.35 V for 3 and 17 h are shown in Fig. 6. The CO-stripping peak at 0.56 V remains practically unchanged in terms of intensity and position, which is different from the behaviour of Pt-2/C. Cathodic polarization at −0.35 V is supposed to reduce the oxygen contents and yet the two catalysts has respond quite differently and this suggests that the activities of the oxygen atoms are not quite the same. The oxygen atoms in Pt-2/C appear to be of an active form, as they respond positively to the hydrogen reduction. The decrease in the number of these 'active' oxygen species by cathodic treatment can account for the observed deterioration of the performance of Pt-2/C.

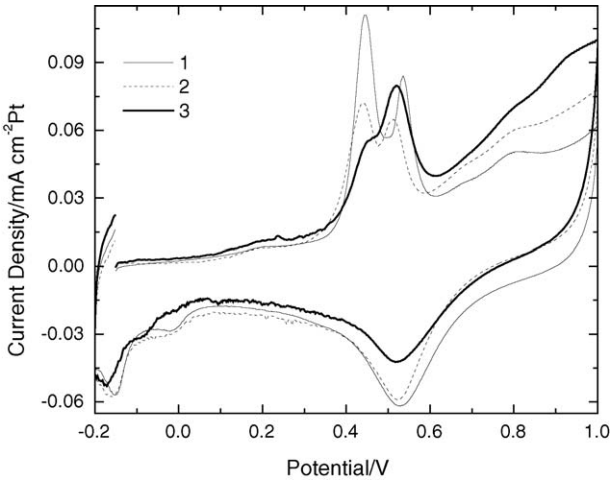

Fig. 5. Room temperature CO-stripping cyclic voltammograms of Pt-2/C in 0.5 M H_2SO_4 at a scan rate of 20 mV s^{-1} (1: no polarization; 2: after polarization at −0.35 V for 3 h; 3: after polarization at −0.35 V for 17 h).

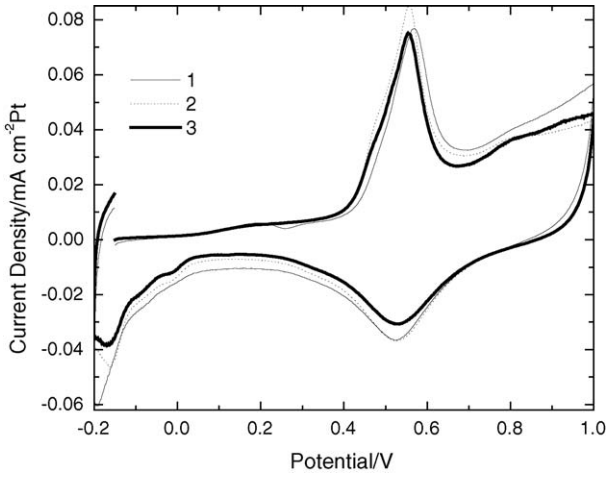

Fig. 6. Room temperature CO-stripping cyclic voltammograms of Pt-1/C in 0.5 M H_2SO_4 at a scan rate of 20 mV s^{-1} (1: no polarization; 2: after polarization at −0.35 V for 3 h; 3: after polarization at −0.35 V for 17 h).

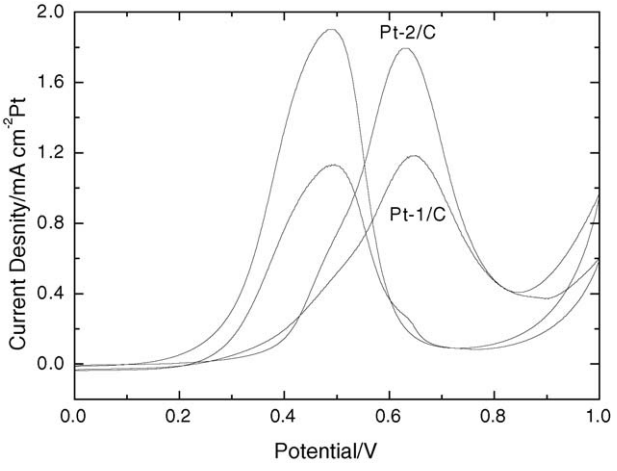

Fig. 7. Catalytic activities for methanol oxidation reaction in 1 M CH_3OH + 0.5 M H_2SO_4 at room temperature (scan rate = 20 mV s^{-1}).

From the voltammograms for room temperature methanol electrooxidation in 1 M CH_3OH + 0.5 M H_2SO_4 (Fig. 7), it is seen that the specific activity of Pt-2/C outperforms that of Pt-1/C by 51%, as determined by the peak current density at ∼0.63 V in the forward scan. It is obvious that Pt-2/C is a better catalyst in terms of specific activity and CO tolerance. More remarkably, these improvements in the methanol oxidation reaction (MOR) are accomplished by a relative simple modification of the method of preparation (i.e., reversal of the mixing sequence of the Pt precursor salt and the reducing agent).

While the Pt nanoparticles in Pt-1/C have all the desirable features according to conventional wisdom, namely, a predominantly metallic state, a narrow particle size distribution and a high state of dispersion on the carbon support, these factors alone are insufficient to ensure good MOR performance. Perhaps the higher oxygen content in Pt-2/C provides a readily accessible source of oxygen, similar to that present on the oxophilic metal sites of a bimetallic catalyst (e.g., PtRu), to react away the adsorbed CO (a catalyst poison) according to the well-known bifunctional catalysis mechanism. At present, the reasons for the improved MOR performance of a more oxidised catalyst such as Pt-2/C are not fully understood, and work is in progress to collect additional facets of this phenomenon. What is assured, however, is the reproducibility of the results from synthesis to application performance measurements when experiments are repeated several times. Despite not knowing the exact reasons, the unusual Pt particle formation route attempted here may open new opportunities in catalyst design for methanol oxidation.

4. Conclusion

In summary, highly catalytically active and CO-tolerant Pt catalysts for the methanol oxidation reaction (MOR) at room temperature have been produced by an unconventional formation route, i.e., by adding the H_2PtCl_6 precursor to a carbon slurry of $NaBH_4$ solution. The experimental results are in apparent disagreement with the established criteria of using a narrow particle-size distribution, a high state of dispersion on the carbon support, and a metallic Pt content, to infer good catalyst performance. While the exact reasons behind the unexpected results are still to be determined, the simplified and highly reproducible preparative method reported here may offer new opportunities in the catalyst design for direct methanol fuel cell applications.

References

[1] S. Wasmus, A. Kuver, J. Electroanal. Chem. 461 (1999) 14–31.
[2] W.C. Choi, J.D. Kim, S.I. Woo, Catal. Today 74 (2002) 235–240.
[3] W.H. Lizcano-Valbuena, D.C.de. Azevedo, E.R. Gonzalez, Electrochim. Acta 49 (2004) 1289–1295.
[4] R. Venkataraman, H.R. Kunz, J.M. Fenton, J. Electrochem. Soc. 150 (2003) A278–A284.
[5] J.H. Zeng, J.Y. Lee, J. Power Sources 140 (2005) 268–273.
[6] O. Levenspiel, Chemical Reaction Engineering, third ed., John Wiley & Sons, New York, 1999, p. 170.
[7] J.M. Solar, C.A. Leon, K. Osseo-Asare, L.R. Radovic, Carbon 28 (1990) 369–375.
[8] Y.C. Liu, X.P. Qiu, Z.G. Chen, W.T. Zhu, Electrochem. Commun. 4 (2002) 550–553.
[9] T.C. Deivaraj, W.C. Chen, J.Y. Lee, J. Mater. Chem. 13 (2003) 2555–2560.
[10] P. Legare, G. Lindauer, L. Hilaire, G. Maire, J.J. Ehrhardt, J. Jupille, A. Gassuto, C. Guillot, J. Lecante, Sur. Sci. 198 (1988) 69–78.
[11] Y.M. Zhu, C.R. Cabrera, Electrochem. Solid-State Lett. 4 (2001) A45–A48.
[12] J.M.D. Rodríguez, J.A.H. Melián, J.P. Pena, J. Chem. Educ. 77 (2000) 1195–1197.
[13] D.C. Papageorgopoulos, M. Keijzer, F.A. de Bruijn, Electrochim. Acta 48 (2002) 197–204.
[14] Z.L. Liu, J.Y. Lee, W.X. Chen, M. Han, L.M. Gan, Langmuir 20 (2004) 181–187.